UCRL-JC-132425
PREPRINT

2-D Electric Fields and Drifts Near the Magnetic Separatrix in Divertor Tokamaks

T. D. Rognlien, D. D. Ryutov, N. Mattor, G. D. Porter

This paper was prepared for submittal to the
40th Annual Meeting of the American Physical Society Division of Plasma Physics
New Orleans, LA
November 16-20, 1998

November 15, 1998

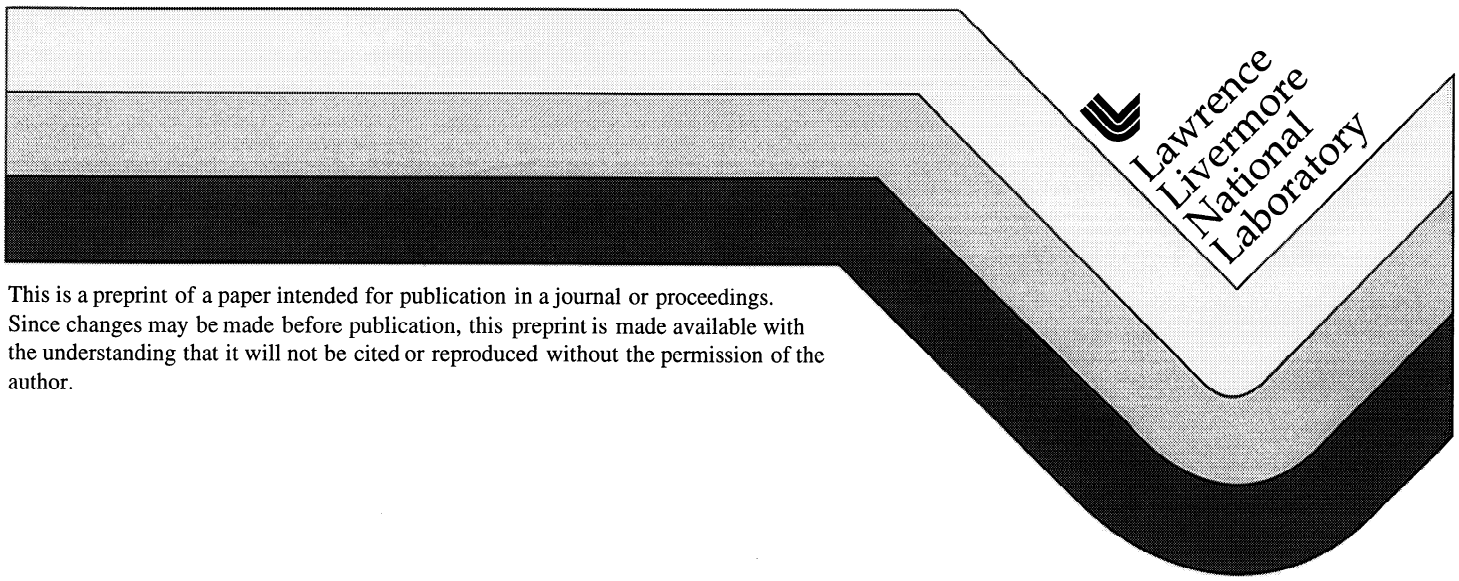

November 15, 1998

2-D electric fields and drifts near the magnetic separatrix in divertor tokamaks

T.D. Rognlien, D.D. Ryutov, N. Mattor, and G.D. Porter
Lawrence Livermore National Laboratory
Livermore, CA 94551

A 2-D calculation is presented for the transport of plasma in the edge region of a divertor tokamak solving continuity, momentum, and energy balance fluid equations. The model uses anomalous radial diffusion, including perpendicular ion momentum, and classical cross-field drifts transport. Parallel and perpendicular currents yield a self-consistent electrostatic potential on both sides of the magnetic separatrix. Outside the separatrix, the simulation extends to material divertor plates where the incident plasma is recycled as neutral gas and where the plate sheath and parallel currents dominate the potential structure. Inside the separatrix, various radial current terms - from viscosity, charge-exchange and poloidal damping, inertia, and ∇B - contribute to the determining the potential. The model rigorously enforces cancellation of gyro-viscous and magnetization terms from the transport equations. The results emphasize the importance of $\mathbf{E}\times\mathbf{B}$ particle flow under the X-point which depends on the sign of the toroidal magnetic field. Radial electric field (E_y) profiles at the outer midplane are small with weak shear when high L-mode diffusion coefficients are used and are large with strong shear when smaller H-mode diffusion coefficients are used. The magnitude and shear of the electric field (E_y) is larger both when the core toroidal rotation is co-moving with the inductive plasma current and when the ion ∇B-drift is towards the single-null X-point.

I. INTRODUCTION

The magnetic separatrix at the edge of a divertor tokamak identifies the boundary between the interior core region where magnetic field lines close on themselves and the outer region where field lines strike material surfaces. In the outer region called the scrape-off layer (SOL), the plasma profiles and electric fields have an inherent 2-D variation assuming toroidal symmetry. On the other hand, well inside the core region, the variation is dominantly radial owing to rapid poloidal transport. The drift velocity caused by the radial electric field is believed important for the reduction of edge turbulence in the pedestal-gradient region via shear giving the L-H mode transport barrier just inside the separatrix,,[1] and for causing asymmetries in the divertor plasma.[2] A thorough summary of recent experimental work on the effect of B-field direction for tokamaks is found in Ref..[3]

As for core transport, edge/SOL transport modeling requires the use of anomalously large radial diffusion coefficients which is believed to arise from plasma turbulence.[1,4] It is thus important to include the effects of both the turbulence and the classical drift velocities in a consistent manner such that the basic properties of the magnetized system such as ambipolarity and no transport from magnetization fluxes are preserved. For example, even though the classical cross-field energy fluxes proportional to temperature gradients as presented in Ref. 5 appear in the as a heat-flux term in the transport equations, their net effect on transport is only proportional to the much smaller ∇B-drift. This type of cancellation is well known and has been discussed by various authors, *e.g.*, Refs. 7,6. A related cancellation that must be accounted for in the momentum equation is the gyroviscosity term with the magnetization momentum flux.[8,9]

In this paper, we present a system of 2-D transport equations which include both anomalous radial diffusion and classical particle drifts for the edge/SOL region, focusing on the self-consistent electrostatic potential and the resulting $\mathbf{E}\times\mathbf{B}$-particle drifts. In Sec. II, the geometry and plasma model are described. In Sec. III, results are presented for the divertor plasma region and the influence of reversing the magnetic field. Also shown are radial electric field profiles near the outer midplane. A summary of the results is presented in Sec. IV.

II. GEOMETRY AND PLASMA MODEL

A. Geometry

We consider the edge-plasma region of a tokamak device as shown in Fig. 1. Toroidal symmetry is assumed, and the 2-D mesh is constructed from the magnetic flux surfaces. The toroidal **B**-field for the "standard" direction, B_z, is out of the paper in the z direction, such that the ion ∇B-drift is downward toward the X-point. The plasma current is taken in the negative z direction giving rise to the poloidal **B**-field component, B_x, in the clockwise direction. The x-coordinate is in the poloidal direction along the flux surface and the y-coordinate is the radial coordinate orthogonal to the flux surface. In addition, the coordinate orthogonal to **B** and lying in the flux surface is called w with unit vector $\hat{\mathbf{i}}_w = -(B_z/B)\hat{\mathbf{i}}_x + (B_x/B)\hat{\mathbf{i}}_z$ (sometimes referred to as the $\perp$-direction). Divertor plates are located at the bottom of device on each side of the magnetic X-point and are the source of recycling gas. In the radial direction, the calculations include a portion of the core-edge plasma well inside the magnetic separatrix.

B. Basic equations

The basic aspects of our edge plasma model are obtained by considering the equations of continuity, momentum, and energy for both the electrons and ions as given by Braginskii.[10] We use SI units. The continuity equations have the form

$$\frac{\partial n_{e,i}}{\partial t} + \nabla \cdot (n_{e,i}\mathbf{v}_{e,i}) = S^p_{e,i} \tag{1}$$

where $n_{e,i}$ and $\mathbf{v}_{e,i}$ are the electron and ion densities and velocities, respectively. The source term $S^p_{e,i}$ arises from ionization of neutral gas and recombination; generally $S^p_e = S^p_i$ for singly ionized plasmas unless a current source such as a probe is present in the plasma.

The momentum equations are given by

$$\frac{\partial n_{e,i} m_{e,i}\mathbf{v}_{e,i}}{\partial t} + \nabla \cdot (m_{e,i} n_{e,i}\mathbf{v}_{e,i}\mathbf{v}_{e,i}) = -\nabla P_{e,i} + q n_{e,i}(\mathbf{E} + \mathbf{v}_{e,i} \times \mathbf{B}) - \mathbf{F}_{e,i} - \mathbf{R}_{e,i} + \mathbf{S}^m_{e,i}. \tag{2}$$

Here m_i is the ion mass, $P_{e,i} = n_{e,i}T_{e,i}$ is the pressure with $T_{e,i}$ being the temperatures, q is the particle charge, **E** is the electric field, **B** is the magnetic field, $\mathbf{F}_{e,i} = \nabla \cdot \mathbf{\Pi}_{e,i}$ is the viscous force, and $\mathbf{R}_{e,i}$ is the thermal force.[10] The source $\mathbf{S}^m_{i,e}$ contains effects of extra momentum exchange with, for example, neutrals.

The ion and electron energy equations can be written in the form

$$\frac{\partial}{\partial t}\left(\frac{3}{2}P_{e,i}\right)+\nabla\cdot\left(\frac{5}{2}\mathbf{v}_{e,i}P_{e,i}+\mathbf{q}_{e,i}\right)=\mathbf{v}_{e,i}\nabla\cdot P_{e,i}-\mathbf{\Pi}_{e,i}\cdot\nabla\mathbf{v}_{e,i}+Q_{e,i}. \tag{3}$$

Here, $\mathbf{q}_{e,i}$ are the heat fluxes, and $Q_{e,i}$ are volume heating terms.[10]

Since anomalous radial transport processes are believed important, we include these in the equations in a systematic manner by allowing enhanced ion and electron collisions frequencies in the classical model as described in detail in Ref. 11 for a slab geometry. This procedure clarifies the role of the diamagnetic fluxes and the radial current driven by anomalous viscosity. In addition, the approach gives us confidence that the diffusive radial fluxes for particles, parallel momentum, and energy preserved the symmetries and conservations laws of the basic system. We assumed that collisions are sufficiently strong to maintain approximately Maxwellian distributions and that the effect of short scale-length turbulence can be described by a diffusion model. Consequently, the form of the anomalous transport coefficients obtained from the slab analysis can be used in a toroidal system provided that the major and minor radii are large compared to the edge plasma scale length.

Because of the parameters typical of edge parameters, a systematic ordering[11] leads to a reduced set of equations. The magnetic field is taken static and given. The electric field comes from $\mathbf{E}=-\nabla\phi$, where ϕ is the electrostatic potential. The equation for ϕ is obtained through the assumption of quasineutrality ($n_i=n_e$) rather than Poisson's equation, where one of the continuity equations, say for n_e, is replaced by the current continuity equation, $\nabla\cdot\mathbf{J}=0$, for ϕ. The only full momentum component included is that of the ions along the magnetic field, $v_{||}$, although the inertialess momentum equations in the w and y directions are used to determine the cross-field velocities. The effects of toroidicity are included by used the guiding-center fluxes for a tokamak geometry. For radial transport, local anomalous transport is assumed to dominate over neoclassical processes from collisional viscosity which is verified *a posteriori.*

The reduced set of five differential equations couples the five unknowns n_i, $v_{||}$, T_e, T_i, and ϕ in the poloidal plane. The detailed form of the equations used for the present study in UEDGE are given in the Appendix where the model for the neutral gas is also given. Note that more complex models for neutrals and nonorthogonal mesh capability do exist for UEDGE as described in Refs. 12 and 13, but here we focus effects of electric fields and cross-field drifts.

1. Perpendicular drifts and currents

The two perpendicular velocity are v_w in the w-direction (or $\perp$-direction) within the flux surface, and the radial v_y. From the momentum equations, Eq. (2), the velocities can be solved for iteratively beginning with the dominant $\mathbf{E}\times\mathbf{B}$ and diamagnetic drifts for ions and electrons

$$v_{w0} = \frac{1}{B}\left(\frac{\partial\phi}{\partial y} + \frac{1}{qn}\frac{\partial P_{i,e}}{\partial y}\right) \equiv v_{w,E} + v_{w,\nabla P} \tag{4}$$

$$v_{y0} = -\frac{1}{B}\left(\frac{\partial\phi}{\partial w} + \frac{1}{qn}\frac{\partial P_{i,e}}{\partial w}\right) - \frac{D_a}{n_{i,e}}\frac{\partial n_{i,e}}{\partial y} \equiv v_{y,E} + v_{y,\nabla P} + v_{y,a} \tag{5}$$

where the ambipolar anomalous diffusive velocity ($v_{y,a} \propto D_a$) is also shown. These velocities give no contribution to $\nabla\cdot\mathbf{J} = 0$ for B constant.[9] The first order corrections to v_y do contribute to $\nabla\cdot\mathbf{J} = 0$ and are given by

$$v_{i,y1} = \frac{1}{n}\left(\frac{1}{eB}\right)^2 \frac{\partial}{\partial y}\eta_{a\perp}\frac{\partial}{\partial y}v_{w0} - \frac{v_{r0}}{\omega_{ci}}\frac{\partial}{\partial y}v_{w0} - \frac{(\nu_{cx}+\nu_{neo})}{\omega_{ci}}v_{w0} + \mathbf{v}_{i,\nabla B}\cdot\hat{\mathbf{i}}_y. \tag{6}$$

In order, these terms arise from anomalous viscosity, inertia, charge-exchange and neoclassical transport, and the guiding-center particle drift from the nonuniform magnetic field. For a tokamak, $B \approx R_0B_0/R$, so for ions and electrons (for example, see Ref. 6)

$$\mathbf{v}_{\nabla B} = \frac{B_z(2P_{i,e} + m_{i,e}nv_{||}^2)}{qB^2R}(\hat{\mathbf{i}}_R\times\hat{\mathbf{i}}_z). \tag{7}$$

This approximation that $v_{\nabla B}$ is vertical is generally very good for tokamaks. For the electrons, the correction to $v_{e,y1}$ is simpler owing to their smaller mass:

$$v_{e,y1} = \mathbf{v}_{e,\nabla B}\cdot\hat{\mathbf{i}}_y. \tag{8}$$

In the x-direction, the corrections reduce to $v_{x1} \approx \mathbf{v}_{\nabla B}\cdot\hat{\mathbf{i}}_x$; the other corrections are much smaller than for v_y, primarily because $|v_{y0}| \ll |v_{w0}|$ and radial gradients are steeper than poloidal gradients.[11]

The equation for the potential is the current continuity equation obtained by subtracting the ion and electron continuity equations and assuming quasineutrality, $n_i = n_e$:

$$\nabla\cdot\mathbf{J}(\phi) = \frac{1}{V}\frac{\partial}{\partial x}\left(\frac{V}{h_x}J_x\right) + \frac{1}{V}\frac{\partial}{\partial y}\left(\frac{V}{h_y}J_y\right) = 0 \tag{9}$$

where the toroidal metric coefficients V, h_x, and h_y are given in the Appendix. Here by $\mathbf{J}$ we mean the currents excluding the magnetization current since the divergence of the latter is automatically

zero owing to it being the curl of a vector.[6] The remaining current components are

$$\mathbf{J} = \left[ne(\mathbf{v}_{i,\nabla B} - \mathbf{v}_{c,\nabla B}) \cdot \hat{\mathbf{i}}_x + J_{||}\frac{B_x}{B}\right]\hat{\mathbf{i}}_x + ne(v_{i,y1} - v_{e,y1})\hat{\mathbf{i}}_y. \tag{10}$$

Note that the terms arising from the $\mathbf{v}_{\nabla B}$-drift do not explicitly depend on ϕ the potential, so they act as source terms in Eq. (9). The expression for the parallel current, $J_{||}$, comes from the electron parallel momentum equation, Eq. (2), ignoring inertia and is

$$J_{||} = \frac{en}{0.51 m_e \nu_e}\frac{B}{B_x}\left(\frac{1}{n}\frac{\partial P_e}{\partial x} - e\frac{\partial \phi}{\partial x} + 0.71\frac{\partial T_e}{\partial x}\right), \tag{11}$$

where ν_e is the electron collision frequency and the numerical coefficients are described in Ref. 10.

2. Boundary conditions

The extended discussion of the boundary conditions at the divertor plates is given elsewhere.[14] We assume that the plasma flows to a perfectly absorbing wall (which are recycled as neutrals). Consequently, we may use zero derivative or "extrapolation" boundary conditions for the density with little change in the solution. For the parallel ion velocity, we use the Bohm sheath condition whose generalization to include $\mathbf{E}\times\mathbf{B}$ drifts given by[7]

$$v_{i||}\alpha + v_{Ew} = \pm \alpha C_s. \tag{12}$$

Here $\alpha \equiv |B_x/B| \ll 1$, $C_s = [(T_e + T_i)/m_i]^{1/2}$ is the ion acoustic speed, and the $\pm$ sign is used at the outer (inner) plate. If the poloidal velocity at the plate exceeds this limit, we use a "slip" condition of $\partial v_{i||}/\partial x = 0$ at the plates

The boundary condition for ϕ, is determined by the sheath potential, ϕ_s. The plate is assumed to be conducting and at a potential, ϕ_p. The potential on the plasma side of the sheath is thus $\phi_p + \phi_s$, where[15]

$$\phi_s = \frac{-T_e}{e}\ln\left[2\sqrt{\pi}\left(\frac{J_{||} - env_{i||} - env_{we}/\alpha}{env_{te}}\right)\right]. \tag{13}$$

where $v_{te} \equiv (2T_e/m_e)^{1/2}$ and $v_{we} = v_{w,E} + v_{w,\nabla P}$ is the perpendicular electron velocity from Eq. (4).

For the energy equations, the boundary conditions at the plates are specified in terms of the energy fluxes in the y-direction, Γ_{Ee} and Γ_{Ei}, which are defined following Eqs. (A6) and (A7) in the Appendix. Neglecting the viscosity, these fluxes are set as follows: $\Gamma_{Ee} = \delta_e n T_e v_{e,x}$ and $\Gamma_{Ei} = \delta_i n T_i v_{i,x}$, where $\delta_i \approx 2$ and $\delta_e \approx \phi_s/T_e + 2 \approx 5$ for Maxwellian distributions.

For the neutral gas which is recycled from incident ions on the divertor plates, the poloidal particle flux is specified as a fraction R_p of the incident ion flux, *i.e.*, $\Gamma_{n,x} = -R_p\Gamma_{i,x}$.

At the radial boundary located at the interface between the edge plasma and the core plasma, here located well inside the separatrix, we specify the density to be a constant, independent of poloidal position. The parallel velocity is taken to have zero radial derivative ($\partial v_{||}/\partial y = 0$), a type of "slip" condition so that $v_{||}$ can take on values consistent with the nearby plasma dynamics, rather than forcing an arbitrary boundary condition. For the energy equations, the power is specified in each of the ion and electron channels, subject to the constraint that T_e and T_i are also constant poloidally.

The potential, ϕ, requires two boundary conditions since it is a fourth order differential equation in y owing to the radial ion velocity (and current) driven by viscosity in Eq. (6). The first condition is that ϕ is a constant poloidally, with the value of the constant set by the condition that there is no net current through this boundary (unless a current source is present). This condition follows directly from integration of Eq. (9) in the periodic x-direction. The second condition on ϕ comes somewhat indirectly. Because the parallel electron conduction is so large, T_e is very nearly a constant in the x-direction in the vicinity of the core boundary. Consequently, one can use the parallel Ohm's law, Eq. (11), with $\partial T_e/\partial x = 0$ to find the x-variation of ϕ on a neighboring flux surface. This determines the radial derivative of ϕ to within a constant, and the constant is determined by the condition that the poloidal-average of the toroidal velocity, v_z, is some specified value called $\bar{v}_z$ or we can use the condition $\partial \bar{v}_z/\partial y = 0$.

On the wall boundaries in the private-flux region below the X-point and the outer wall, we use a density-gradient scale-length of 2 cm. As at the core boundary, for $v_{||}$ we use $\partial v_{||}/\partial y = 0$. The values of $T_{e,i}$ are set to 2 eV. For ϕ, two conditions are again needed because of the radial derivatives in J_y, but here the potential is dominated by the parallel currents. Thus, $E_y = 0$ and $\partial E_y/\partial y = 0$ are used to impose minimal constraints on the ϕ in this region.

III. RESULTS OF TRANSPORT SIMULATIONS

In this section, we present a series of results from simulations from the UEDGE code to illustrate the role of classical cross-field drifts on both the divertor region plasma and on the core/SOL boundary region near the outer midplane. The basic DIII-D geometry shown in Fig. 1 is used. The

parameters of these calculations are a core-edge density of 3×10^{19} m^{-3}, a total power of 1.5 MW split equally between ions and electrons. The recycling coefficient is $R_p = 0.90$ to 0.98. We use anomalous radial diffusion coefficients ranging from 0.25-1.0 m^2/s, but we generally keep all the same value which we denote simply as D. Explicitly, the separate coefficients are $D_a, \eta_{a||}, \eta_{a\perp}, \chi_e$, and χ_i for density, parallel ion velocity, perpendicular ion velocity, electron energy, and ion energy, respectively. For calculating the potential, we find that the radial current arising from Eq. (6) is dominanted by the anomalous viscosity and ∇B terms compare to the charge-exchange and neoclassical terms discussed elsewhere.[16]

A. Influence of drifts on the divertor plasma

Recently, we showed the effects of reversal of B_z for the case corresponding to $R_p = 0.95$ and $D = 0.5$ on the density and temperatures at the inner and outer divertor plates and the particle flow.[17] It was shown for these parameters that the $\mathbf{E}\times\mathbf{B}$ flow under the X-point is largely responsible for the substantial plate density and temperature changes with the reversal of B_z. This effect can be understood from the radial electric field that arises in the private flux region owing to the drop in T_e in moving down from the X-point (see Fig. 1). This electric field points downward below the X-point, and so for positive B_z particles $\mathbf{E}\times\mathbf{B}$-drift from the outer divertor to the inner divertor below the X-point. Upon changing B_z to a negative value, the drift reverses, and the corresponding flow is towards the outer divertor. For these cases, the $\mathbf{E}\times\mathbf{B}$ flow under the X-point dominants the oppositely directed $\mathbf{E}\times\mathbf{B}$ flow in the SOL region.

We have repeated these calculations for at range of recycling coefficients from $R_p = 0.9$ to 0.98. As for the case just describe, we use the inner-core boundary condition of $\partial\bar{v}_z/\partial y = 0$, so no core source of toroidal momentum is assumed. The qualitative behavior is the same as just described, with the ratio of T_e for positive to negative B_z increasing at lower R_p, reaching a value of 2.9 eV / 14.4 eV on the inner plate for $R_p = 0.9$. The corresponding density ratio is 1.8e20/0.5e20. The outer plate is less sensitive to the sign of B_z, but has the opposite trend to the inner plate. As R_p is increased toward 0.98, the divertor plasma detaches on both inner and outer plates, with the inner plate detaching much earlier for B_z positive, and only marginally sooner for B_z negative. Once detached, the flow in the private flux region is more complicated, and does not show a simple reversal with the sign of B_z.

The case of $R_p = 0.9$ corresponds to low rather divertor density, similar to conditions obtained in the JET tokamak where Langmuir probe measurements were made of the parallel current on each divertor plate.[18] We show the resulting parallel current density obtained from our simulations in Fig. 2 for the inner and outer divertor plates for each sign of B_z. Here the current sign convention is that the current density flowing *into* each plate is plotted as positive. Therefore, for the upper set of two plots corresponding to positive B_z, a current flows in the SOL from the hotter outer plate to the cooler inner plate as expected. However, in the private-flux region, outer plate current changes sign, just as found in the experiment.[18] For the negative B_z case, the current as does not follow the simple hotter-to-colder direction for the thermoelectric. Again, much of the qualitative structure corresponds to the JET data. For a closer comparison, the reader is referred to Figs. 3 and 4 of Ref.18.

B. Electric field profiles at the core/SOL interface

The electric field at the core/SOL boundary can change dramatically with changes in the toroidal velocity at the core-boundary, $\bar{v}_z$, and with the anomalous diffusion coefficients. The profile of E_y at the outer midplane is shown in Fig. 3, for two values of $\bar{v}_z$, both for forward and reversed B_z. The label of $L_\phi = \pm 1$ in the figure corresponds to a toroidal velocity of $\bar{v}_z = \mp 12$ km/s at the interior core boundary of our simulation. Thus, $L_\phi = +1$ means that the assumed source of the core rotation, the neutral beams, are injected in the same direction as the plasma current. The intermediate case labeled $L_\phi = 0$ corresponds to using the "slip" boundary condition $\partial \bar{v}_z / \partial y = 0$. These result predict that the magnitude and shear in the radial electric field, E_y, is largest for negative L_ϕ, corresponding to counter-injection of the neutral beams. There is experimental evidence that the L-H mode power threshold is somewhat lower for counter-injection,[19] which qualitatively fits the notion of E_y shear stabilization of turbulence.[1] For negative B_z, the E_y well is shallower, again qualitatively in the correct sense for the higher L-H mode power threshold this case.

The calculated strength of E_y is also strongly dependent on the magnitude of the anomalous radial diffusion. In Fig. 4a, we show the effect on E_y of changing the value of all of the anomalous diffusion coefficients; $D = 0.25$ m^2/s can be thought of as H-mode-like values and $D = 1.0$ m^2/s as L-mode values. The edge plasma is self-consistently evolved to equilibrium profiles with the UEDGE code, and the corresponding electron temperature profiles are plotted in Fig. 4b. One sees that there is a sensitive connection between between lowering the diffusion and developing

a strong E_y well through changes in the plasma profiles. In should be noted although all of the anomalous coefficients are changed together, the strongest influence comes from $\chi_{e,i}$ for energy transport. Changing the anomalous viscosity, $\eta_{a\perp}$, has a fairly small effect since plays the role of connecting the core-edge and the SOL through the separatrix boundary-layer.

A more detailed understanding of the E_y profiles in the cases of $D = 1$ m^2/s and $D = 0.25$ m^2/s can be obtained from Fig.5 where the different components are plotted. From the radial ion momentum equation in lowest order, one can obtain the oft-used expression for E_y:

$$E_y = \frac{\partial P_i}{\partial qn} + v_{ix}B_z - v_{iz}B_x \tag{14}$$

Because our simulation evolves v_{ix} and v_{iz} self-consistently, we can use these to understand the details. From Fig.5, it is clear that the ion pressure plays a major role in increasing the magnitude of E_y, an anticipated result since the lower value of D naturally leads to a larger gradient. But one also sees that the poloidal velocity, vix, plays an important role in providing a large amount of the shear in E_y.

IV. SUMMARY

We have presented a model for 2-D edge-plasma transport in tokamaks which includes anomalous radial diffusion transport and classical cross-field drifts. Toroidal symmetry is assumed and five differential equations are solved for the variables n_i, $v_{||}$, T_e, T_i, and ϕ. The model rigorously enforces cancellation of gyro-viscous and magnetization terms from the transport equations and requires the anomalous terms to mimic classical transport in order to preserve basic properties of the ion-electron sytem. The potential is solved across the separatrix where anomalous radial transport of ion momentum is the dominate source of radial current depending directly on the potential, ϕ.

In the divertor region, we find that $\mathbf{E}\times\mathbf{B}$ flow under the X-point is the dominate source of inner/outer divertor asymmetry upon reversal of the toroidal field, B_z. The relative effects are stronger for attached plasma and in determining the detached plasma boundary as parameters are varied. The structure and magnitude of the currents calculated at the divertor plates are in rough agreement with measurements in JET.[18]

The shape and magnitude of the radial electric field, E_y, at the midplane is found to be sensitive to both the assumed toroidal rotation of the core plasma at the inner core-edge boundary and the

size of the anomalous diffusion coefficients. Co-rotation of the core ions with the plasma current gives a weaker E_y than counter injection, suggesting better stabilization of edge turbulence for the latter case. The self-consistent evolution of the edge profiles shows that large magnitude and shear of E_y occurs at low diffusion coefficients, with the shear coming largely from the shear in the poloidal velocity component.

ACKNOWLEDGMENTS

Work performed under the auspices of the USDOE by the Lawrence Livermore National Laboratory under contract number W-7405-ENG-48. We are pleased to acknowledge useful conversations with R.H. Cohen, S.I. Krasheninnikov, M.E. Rensink, R. Schneider, and X.Q. Xu.

Appendix A. Detailed equations used for the simulations

The basic form of the transport equations without cross-field drifts corresponds to that given for a number of edge transport codes being based on classical fluid equations, one of the first being the B2 code as later specified in Ref. 20. Here we show the modifications to this equation set as used in UEDGE when classical cross-field drifts are included. The plasma velocities in our equations are denoted by the symbol **u** and differ from the total velocities in the fluid equations by having the classical cross-field pressure or temperature gradient terms omitted since these have zero divergence, or cancel with gyro-viscous terms, and therefore do not contribute to the transport.[6,11] Note that $v_{||} = u_{||}$. For the poloidal ion velocity

$$u_{ix} = \frac{B_x}{B} v_{i||} + v_{x,E} + v_{ix,\nabla B}, \tag{A1}$$

where the x-component of $v_{i,\nabla B}$ comes directly from Eq. (7). For the radial ion velocity

$$u_{iy} = -\frac{D_a}{n_i}\frac{\partial n_i}{\partial y} + v_{y,E} + v_{iy,vis} + v_{iy,\nabla B}, \tag{A2}$$

where the last two terms come from the corrections to $v_{i,y1}$ given in Eq. (6).

The electron velocities are obtained from

$$\mathbf{u}_e = \frac{n_i Z_i \mathbf{u}_i}{n_e} - \frac{(\mathbf{J}_{||} + \mathbf{J}_{vis} + \mathbf{J}_{\nabla B})}{e n_e}. \tag{A3}$$

The ion continuity equation

$$\frac{\partial}{\partial t}(n_i) + \frac{1}{V}\frac{\partial}{\partial x}(\frac{V}{h_x} n_i u_{ix}) + \frac{1}{V}\frac{\partial}{\partial y}(\frac{V}{h_y} n_i u_{iy}) = (\langle \sigma_i v_e \rangle - \langle \sigma_r v_e \rangle) n_e n_n \tag{A4}$$

The terms $\langle \sigma_r v_e \rangle$ and $\langle \sigma_i v_e \rangle$ are rate coefficients for recombination and ionization, respectively. The metric coefficients are $h_x \equiv 1/||\nabla x||$, $h_y \equiv 1/||\nabla y||$, and $V = 2\pi R h_x h_y$ is the volume element for toroidal geometry with major radius R.[20] For brevity of presentation, the metric coefficients are suppressed in the remaining equations.

The ion parallel momentum equation

$$\frac{\partial}{\partial t}(m_i n_i u_{i||}) + \frac{\partial}{\partial x}\left(m_i n_i u_{i||} u_{ix} - \eta_x \frac{\partial v_{i||}}{\partial x}\right) + \frac{\partial}{\partial y}\left(m_i n_i v_{i||} u_{iy} - \eta_{ya} \frac{\partial v_{i||}}{\partial y}\right) = \frac{B_x}{B}\left(-\frac{\partial P_p}{\partial x}\right) \tag{A5}$$

where $P_p = P_e + P_i$, η_x is the classical viscosity, $\eta_x = (B_x/B)^2 \eta_{||}$, and η_{ya} is anomalous. All classical viscosities and thermal conductivities are flux-limited to prevent unphysically large values in any regions with long mean-free paths.

The electron energy equation

$$\frac{\partial}{\partial t}\left(\frac{3}{2}n_eT_e\right)+\frac{\partial}{\partial x}\left[\frac{5}{2}n_eu_{ex}T_e-\kappa_{ex}\frac{\partial T_e}{\partial x}-0.71n_eT_e\frac{B_x}{B}\frac{J_{||}}{en_e}\right]+\frac{\partial}{\partial y}\left(\frac{5}{2}n_eu_{ey}T_e-\kappa_{ey}\frac{\partial T_e}{\partial y}\right)$$
$$=u_{ix}\frac{\partial P_e}{\partial x}-u_{iy}\frac{\partial P_i}{\partial y}-u_{iw}\frac{B_x}{B}\frac{\partial P}{\partial x}+\mathbf{E}\cdot\mathbf{J}-K_q(T_e-T_i)+S_{Ee}. \tag{A6}$$

Here the poloidal heat conductivity is classical, $\kappa_{ex}=(B_x/B)^2=\kappa_{||}$, radial is anomalous, $\kappa_{ey}=n\chi_e$, and K_q is the collisional energy exchange coefficient.

The ion energy equation

$$\frac{\partial}{\partial t}\left(\frac{3}{2}n_iT_i\right)+\frac{\partial}{\partial x}\left[\frac{5}{2}n_iu_{ix}T_i-\kappa_{jx}\frac{\partial T_i}{\partial x}\right]+\frac{\partial}{\partial y}\left(\frac{5}{2}n_iu_{iy}T_i-\kappa_{jy}\frac{\partial T_i}{\partial y}\right)=\mathbf{u}_i\cdot\nabla p_i$$
$$+\eta_{ix}\left(\frac{\partial v_{ij||}}{\partial x}\right)^2+\eta_{iy}\left(\frac{\partial v_{i||}}{\partial y}\right)^2+K_{qj}(T_e-T_i)+\frac{1}{2}m_iv_{i||}^2n_i\nu_{iz}+S_{Ej}. \tag{A7}$$

As for the electrons, the poloidal thermal conduction (and viscosity) coefficients are classical and the radial are anomalous. The energy fluxes in the square brackets in of Eqs. (A6) and (A7) are denoted Γ_{Ee} and Γ_{Ei}, respectively, and are used to define the energy boundary conditions are the divertor plates in Sec. II; note that cross-field energy flux terms proportional to temperature gradients which do properly appear in Ref. 10, are omitted here since these fluxes have zero divergence except for that convected by $\mathbf{v}_{\nabla B}$.

The current continuity equation, $\nabla\cdot\mathbf{J}(\phi)=0$, used to calculate the potential is given by Eqs. (9) and (10). Note that the expression for the radial current is very different from that in Ref. 20.

For the calculations reported in this paper, we use a simplified diffusive model of the neutral transport where

$$\mathbf{v}_n=-\frac{\nabla(n_nT_n)}{m_in_n(n_i\langle\sigma_{cx}v_i\rangle+n_e\langle\sigma_iv_e\rangle)}. \tag{A8}$$

The neutral gas density, n_g, is determined by solving the continuity equation

$$\frac{\partial}{\partial t}(n_n)+\frac{\partial}{\partial x}(n_nv_{nx})+\frac{\partial}{\partial y}(n_nv_{ny})=(\langle\sigma_rv_e\rangle-\langle\sigma_iv_e\rangle)n_en_n. \tag{A9}$$

References

[1]K.H. Burrell, Phys. Plasmas **4**, 1499 (1997).

[2]I.H. Hutchinson, *et al.*, Plasma Phys. Contr. Fusion **37**, 1389 (1995).

[3]K. Ida, Plasma Phys. Contr. Fusion **40**, 1429 (1998).

[4]X.Q. Xu and R.H. Cohen, Contrib. Plasma Phys. **38**, 158 (1998).

[5]F.L. Hinton and G.M. Staebler, Nucl. Fusion **29**, 405 (1989).

[6]A.V. Chankin, J. Nucl. Mater. **241-243**, 199 (1997).

[7]R.H. Cohen and D.D. Ryutov, Comments Plasma Phys. Controlled Fusion **16**, 255 (1995).

[8]F.L. Hinton and Y.-B. Kim, Nucl. Fusion **34**, 899 (1994).

[9]T.D. Rognlien and D.D. Ryutov, Contrib. Plasma Phys. **38**, 152 (1998).

[10]Braginskii, S.I., Transport processes in a plasma *Reviews of Plasma Physics*, Vol. I, Ed. M.A. Leontovich (Consultants Bureau, New York, 1965), p. 205.

[11]T.D. Rognlien and D.D. Ryutov, "Pseudo-classical transport equations for the tokamak edge plasma in the slab approximation," LLNL Report, Nov. 1998.

[12]T.D. Rognlien, B.J. Braams, and D.A. Knoll, Contrib. Plasma Phys. **36**, 105 (1996).

[13]F. Wising, D.A. Knoll, S. Krasheninnikov, T.D. Rognlien, and D.J. Sigmar, Contrib. Plasma Phys. **36**, 136 (1996).

[14]R.H. Cohen and D.D. Ryutov, Invited talk, DPP-APS meeting, Nov. 16-20, 1998 (New Orleans).

[15]R.H. Cohen and D.D. Ryutov, Phys. Plasmas **2**, 2011 (1995).

[16]B.A. Carreras, L.W. Owen, R. Maingi, *et al.* Phys. Plasma **5**, 2623 (1998).

[17]T.D. Rognlien, G.D. Porter, and D.D. Ryutov, J. Nucl. Mater., accepted for pub. (1998).

[18]M.J. Schaffer, A.V. Chankin, H.Y. Guo, *et al.*, Nucl. Fusion **37** (1997) 83.

[19]D.P. Schissel, S.L. Allen, K.H. Burrell, *et al.*,, Phys. Fluids B **1**, 1843, (1989).

[20]B.J. Braams, Contrib. Plasma Phys. **36**, 276 (1996).

Figures

FIG. 1. The poloidal plane of the DIII-D tokamak showing the edge region being simulated. The magnetic flux-surface mesh is shown to illustrate the coordinates: x is along the flux surface and y is orthogonal to the flux surface. The w coordinate shown is perpendicular to $\mathbf{B}$, and lies in the flux surface, slight out of the poloidal plane. The directions of the B-field components and plasma current, I_p, correspond to typically operating conditions for DIII-D.

FIG. 2. The parallel current density on the inner and outer divertor plates for the low density case of $R_p = 0.9$ for both signs of the toroidal field, B_z. Positive current means current directed into the plate on each side.

FIG. 3. Radial electric field, E_y, versus radius at the outer midplane for three different toroidial momentum boundary conditions at the interior core boundary. Here $L_\phi = 1$ corresponds to co-injection of the neutral beams with the plasma current at a level giving $\bar{v}_z = -12$ km/s, and the opposite for $L_\phi = -1$. For $L_\phi = 0$, $\partial \bar{v}_z / \partial y = 0$ is used.

FIG. 4. Midplane plots of a), radial electric field, E_y, for different anomalous diffusion coefficients, and b), electron temperature. Units of D are m^2/s.

FIG. 5. Components of the radial electric field from the radial ion force balance equation. Here a) has $D = 1.0$ m^2/s, and b) has $D = 0.25$ m^2/s

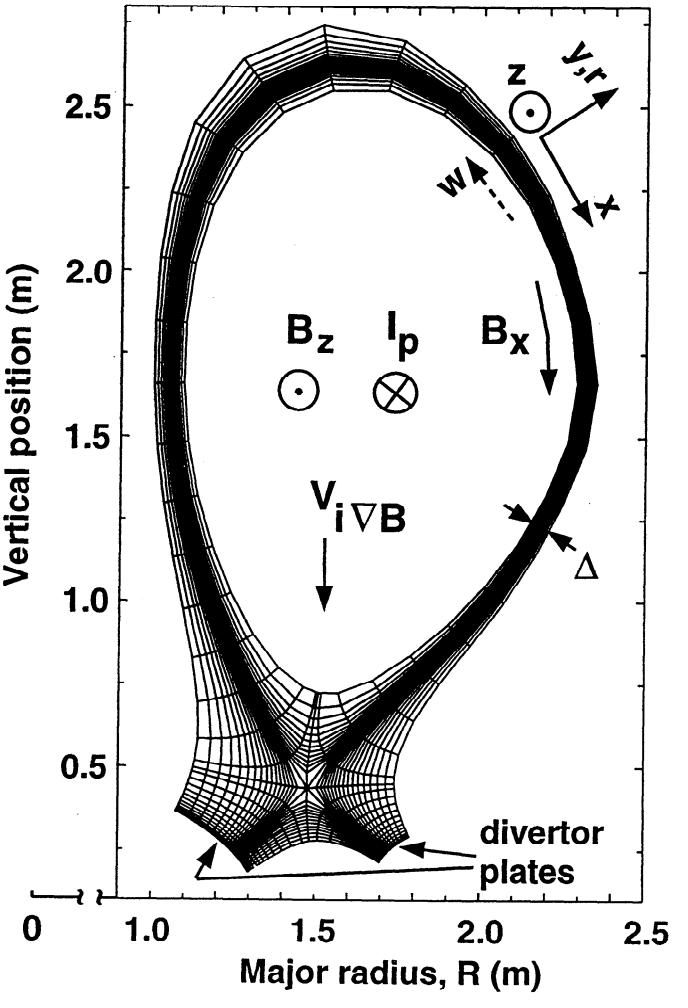
z
v_{ir}
w
x
B_z
I_p
B_x
$V_i \nabla B$
Δ
divertor
plates
Vertical position (m)
2.5
2.0
1.5
1.0
0.5
0
1.0
1.5
2.0
2.5
Major radius, R (m)

Fig. 1

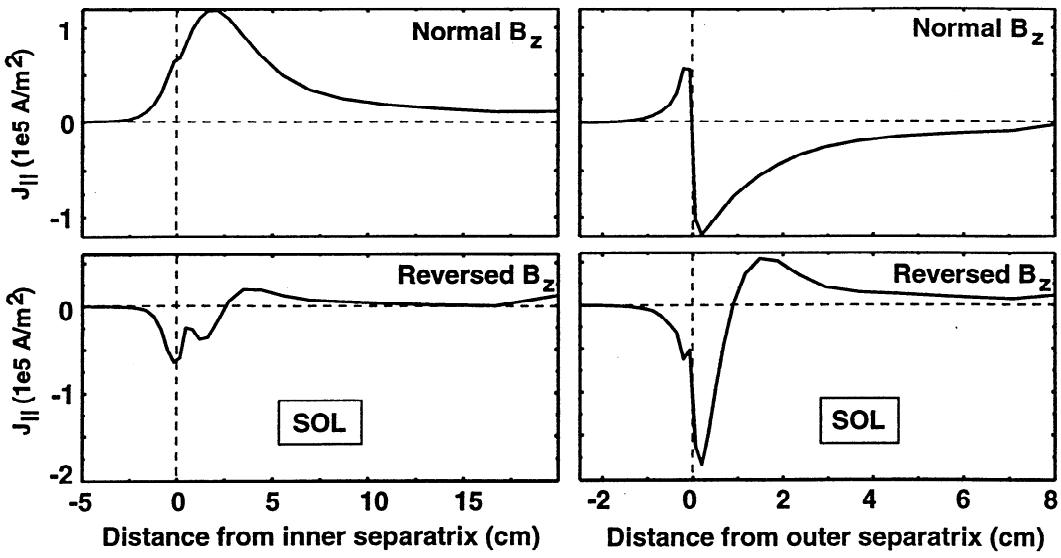
Normal B_z
Normal B_z
Reversed B_z
Reversed B_z
SOL
SOL
$J_{||}$ (1e5 A/m^2)
$J_{||}$ (1e5 A/m^2)
1
0
-1
0
-1
-2
-5
0
5
10
15
-2
0
2
4
6
8
Distance from inner separatrix (cm)
Distance from outer separatrix (cm)

Fig. 2

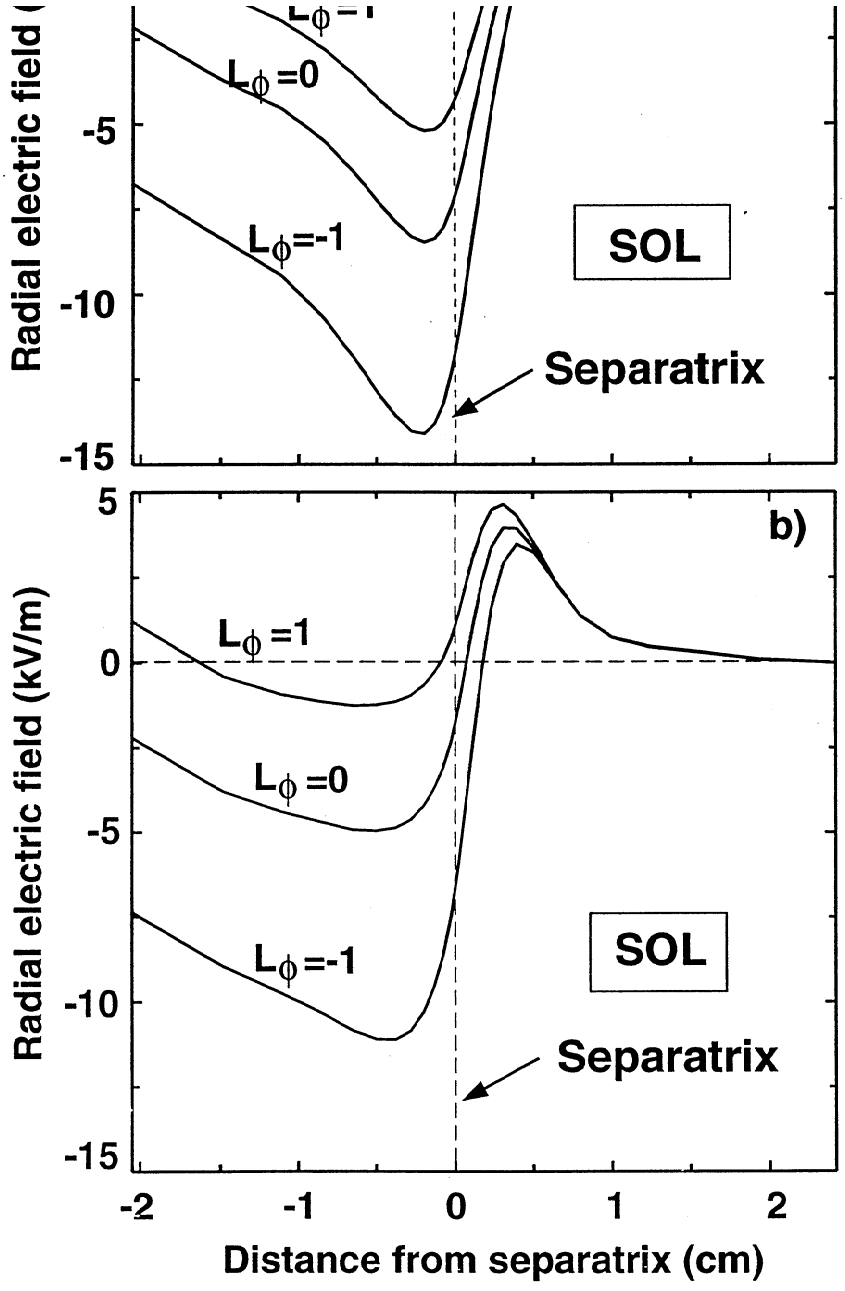
Radial electric field (
-5
-10
-15
Lϕ=0
Lϕ=-1
SOL
Separatrix
5
0
-5
-10
-15
b)
Lϕ=1
Lϕ=0
Lϕ=-1
SOL
Separatrix
Radial electric field (kV/m)
-2
-1
0
1
2
Distance from separatrix (cm)

Fig. 3

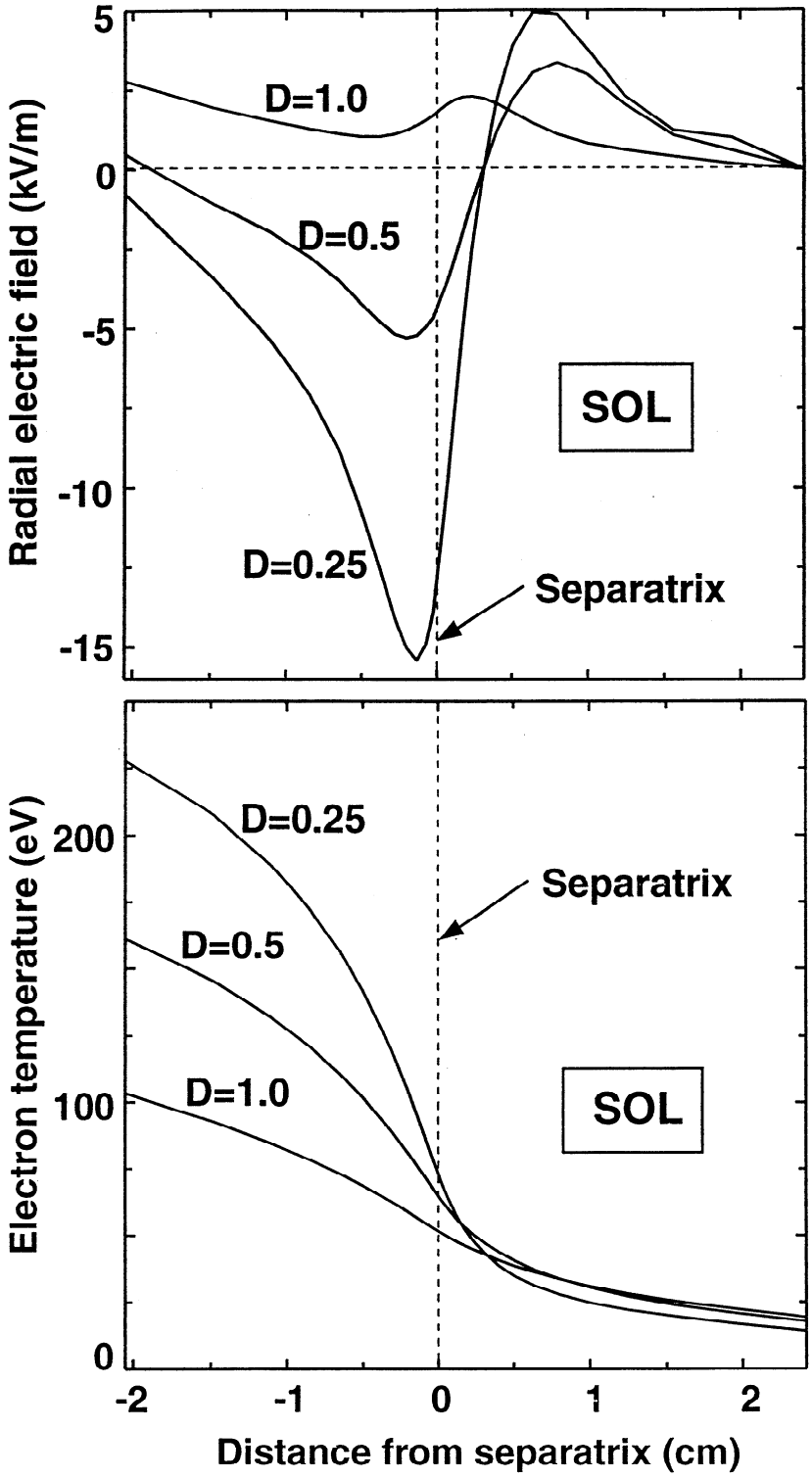
Radial electric field (kV/m)
5
0
-5
-10
-15
D=1.0
D=0.5
D=0.25
SOL
Separatrix
Electron temperature (eV)
200
100
0
D=0.25
D=0.5
D=1.0
Separatrix
SOL
-2
-1
0
1
2
Distance from separatrix (cm)

Fig. 4

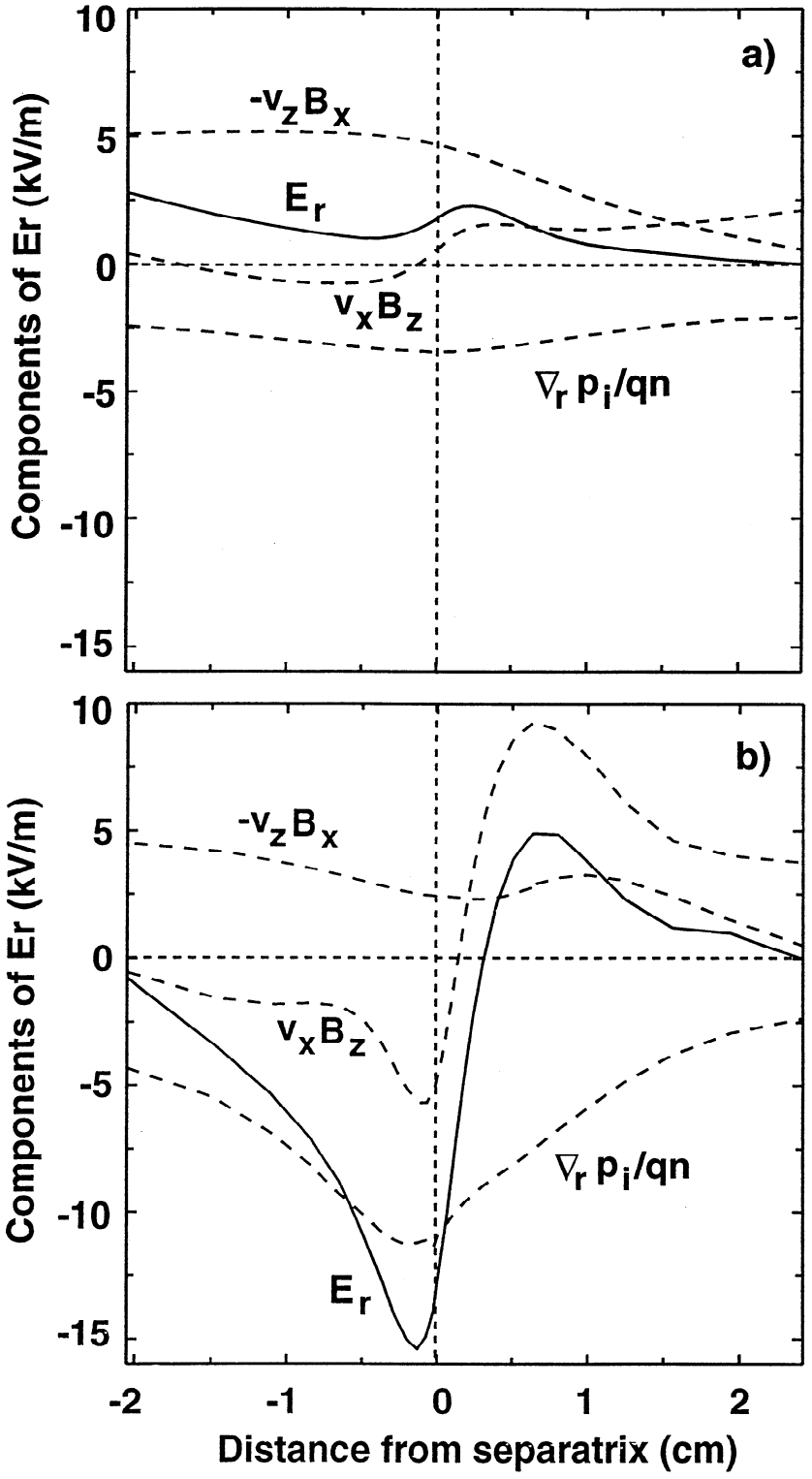
a)
b)
$-v_z B_x$
E_r
$v_x B_z$
$\nabla_r p_i/qn$
Components of Er (kV/m)
Distance from separatrix (cm)
10
5
0
-5
-10
-15
-2
-1
0
1
2

Fig. 5